Kinetics and Catalysis, Vol. 41, No. 1, 2000, pp. 132–144. From Kinetika i Kataliz, Vol. 41, No. 1, 2000, pp. 148–160.

Bifunctional Catalysis of Mo/HZSM-5 in the Dehydroaromatization of Methane with CO/CO_2 to Benzene and Naphthalene[1, 2]

S. Liu, L. Wang***, R. Ohnishi*, and M. Ichikawa***

** Catalysis Research Center, Hakkaido University, Kita-Ku, N-11, W-10, Sapporo O-60, Japan; e-mail: michi@cat.hokudai.ac.jp*

*** Hebei University of Science and Technology, Shijiazhuang 050018, China*

**** Dalian Institute of Chemical Physics, Dalian, China*

Received December 15, 1998

Abstract—The catalytic dehydrocondensation of methane to aromatics such as benzene and naphthalene was studied on the Mo carbide catalysts supported on micro- and mesoporous materials such as HZSM-5 (0.6 nm) and FSM-16 (2.7 nm). The Mo catalysts supported on H-ZSM-5 having appropriate micropores (0.6 nm size) and Si/Al ratios (20–70) exhibit higher yields (90–150 nmol/g-cat/s) and selectivities (higher than 74% on the carbon basis) in methane conversion to aromatic products such as benzene and naphthalene at 973 K and 1 atm, although they are drastically deactivated because of substantial coke formation. It was demonstrated that the CO/CO_2 addition to methane effectively improves the catalyst performance by keeping a higher methane conversion and selectivities of benzene formation in the prolonged time-on-stream. The oxygen derived from CO and CO_2 dissociation suppresses polycondensation of aromatic products and coke formation in the course of methane conversion. XAFS and TG/DTA/mass-spectrometric studies reveal that the zeolite-supported Mo oxide is endothermally converted under the action of methane around 955 K to nanosized particles of molybdenum carbide (Mo_2C) (Mo–C, coordination number = 1, R = 2.09 Å; Mo–Mo, coordination number = 2.3–3.5; R = 2.98 Å). The SEM pictures showed that the nanostructured Mo carbide particles are highly dispersed on and inside the HZSM-5 crystals. On the other hand, it was demonstrated by IR measurements of pyridine adsorption that the Mo/HZSM-5 catalysts having the optimum SiO_2/Al_2O_3 ratios around 40 show the maximum Brönsted acidity among the catalysts with the SiO_2/Al_2O_3 ratios of 20–1900. There is a close correlation between the activity of benzene formation in the methane aromatization and the Brönsted acidity of HZSM-5 due to the bifunctional catalysis.

INTRODUCTION

The catalytic conversion of methane to petrochemical feed stock such as ethylene and benzene has been of current importance and industrial interest in the effective utilization of carbon resources of natural gas. Several one-step catalytic processes converting methane to valuable products have been studied during the past 20 years, including the oxidative coupling of methane (OCM) to ethene (or ethane), selective oxidation of methane to methanol/formaldehyde, and the homologation of methane to lower hydrocarbons [1–6]. Nevertheless, the industrial interests in these processes have been limited so far because of a low product selectivity at a higher conversion of methane. During the past five years, the nonoxidative conversion of methane to benzene has been reported by Wang, Xu and Guo [7, 8], Solymosi [9–12], and Lunsford [16, 17] on HZSM-5 zeolite-supported Mo catalysts in conjunction with their reactivities, reaction mechanism, and catalyst characterization by XPS [10, 12], XRD, and NMR [13, 14]. Recent works by Ichikawa *et al.* [18, 19] demonstrated that methane with CO and/or CO_2 is catalytically converted into aromatics such as benzene and naphthalene with hydrogen evolution on Mo/HZSM-5 and Fe/Co promoted Mo/HZSM-5 at 873–973 K with the remarkably stable activity.

This paper will present the kinetics of methane conversion with CO/CO_2 to aromatic products such as benzene by varying the methane pressure and flow rates on Mo/HZSM-5 and Fe/Co modified Mo/HZSM-5 catalysts. We will discuss the promotion role of CO/CO_2 addition to methane with the purpose to effectively reduce the coke formation and the improve the catalyst stability. We evaluated carefully the activities and selectivities of methane conversion to aromatics and coke formation on the Mo-supported catalysts. The Mo/HZSM-5 catalysts are characterized by EXAFS/SEM and TG/DTA/mass-spectrometry for the carburization of Mo oxide on HZSM-5 with methane toward Mo_2C. The bifunctional role of molybdenum carbide and HZSM-5 zeolite is discussed in conjunction with the active states of Mo and Brönsted, and the

[1] This article was submitted by the authors in English.

[2] Presented at III Seminar on the Theoretical Problems of the Catalytic Conversion of C_1 Molecules in Chernogolovka, September 28–October 2, 1998.

0023-1584/00/4101-0132$25.00 © 2000 MAIK "Nauka/Interperiodica"

Lewis acidity function of HZSM-5 supports having different Si/Al ratios.

EXPERIMENTAL

Materials and Catalyst Preparation

The Mo-supported catalysts were prepared using either an incipient wetness or a conventional impregnation method. The materials used were as follows: $(NH_4)_6Mo_7O_{24} \cdot 4H_2O$ (Kanto Chem. Co.), NH_4ZSM-5 zeolite (SiO_2/Al_2O_3 = 20–1900; specific surface area, 780–925 m^2/g; Toso Co. and CRI Zeolyst, Inc., as purchased) and FSM-16 (gifted from Toyota Central Research Lab.; pore size = 2.7 nm; SiO_2/Al_2O_3 = 320; specific surface area 980 m^2/g). The Al contents in the HZSM-5 and FSM-16 supports were analyzed by ICP measurements of the samples dissolved with an HF solution. The 3–6 wt % Mo loading Mo/HZSM-5 catalysts were prepared by impregnation of NH_4ZSM-5 with $(NH_4)_6Mo_7O_{24} \cdot 4H_2O$ (Kanto Co., as purchased) from an aqueous solution. The resulting materials were dried at 393 K and calcined at 773 K for 6 h by the monolayer dispersion technique, as reported for $AuCl_3$/NaY zeolite in the literature [18]. Powdered Mo carbide (Mo_2C; 1.8 μm size; specific surface area, 1–2 m^2/g) was purchased from Japan New Metal Co. and was used as received.

Catalytic Measurements and Product Analysis

The catalytic tests were carried out under atmospheric pressure of methane in a continuous flow system with a quartz reactor 8 mm in diameter which was charged with 0.30 g of the pelleted catalyst and sized to 20–42 mesh. The outlet pipe line from the reactor and the on-line sampling valve were kept at a temperature higher than 500 K to prevent the condensation or strong adsorption of the heavy hydrocarbon products. The feed gas mixture of 98% CH_4 (99.9% purity) and 2% Ar (Daido Hokusan Gas Co.; 99.9% purity) as an internal standard for analysis was introduced into the reactor at 7.2 ml/min controlled with a mass flow controller (Brooks Co.) after flushing with He at 973 K for 40 min. The Shimadzu GC-14A gas chromatograph with a flame ionization detector (FID) was equipped with a 6-way valve heated to 260°C for sampling and separation of hydrocarbon products, including nonvolatile compounds such as benzene derivatives and naphthalene on a 4 mm × 1 m Porapak-P column. Another Shimadzu GC-8A chromatograph was employed for on-line analysis of H_2, Ar, CO, CH_4, and CO_2 on a 4 mm × 2 m activated carbon column with a thermal conductivity detector (TCD). C_6–C_{12} condensable materials such as benzene, toluene, xylene, naphthalene, and methylnaphthalene were identified by on-line GC and GC-MS (Perkin-Elmer 910 Q-Mass spectrometer).

The total gas flow rate at the inlet and outlet of the reactor can be described by equation (1), since the mass flow rate of Ar as an internal standard gas should be constant through the reaction progress. Conversion of methane and selectivity to each product containing a carbon atom including CO and CO_2 on the carbon basis ($S^C_{product}$) were calculated from equations (2) and (3), respectively.

$$F^{in}X^{in}_{Ar} = F^{out}X^{out}_{Ar}, \tag{1}$$

$$\alpha = \frac{F^{in}X^{in}_{CH_4} - F^{out}X^{out}_{CH_4}}{F^{in}X^{in}_{CH_4}} = 1 - \frac{X^{out}_{CH_4}X^{in}_{Ar}}{X^{in}_{CH_4}X^{out}_{Ar}}, \tag{2}$$

$$S^C_{product} = \frac{F^{out}X^{out}_{product}N^C_{product}}{F^{in}X^{in}_{CH_4} - F^{out}X^{out}_{CH_4}} = \frac{X^{in}_{Ar}X^{out}_{product}N^C_{product}}{X^{out}_{Ar}X^{in}_{CH_4} - X^{in}_{Ar}X^{out}_{CH_4}}. \tag{3}$$

In these equations, F^{in}, F^{out}, X, and N_C represent the total gas flow rate, mole fraction, and carbon number in a molecule, respectively. Similarly, the selectivity for the formation of a hydrogen-containing product on the hydrogen basis can be calculated; thus, the ratio of hydrogen to carbon in the coke formed can be estimated.

Thus, the selectivity for coke formation on the carbon basis was calculated as (1) the sum of product selectivities ($1 - \sum S^C_{product}$). Coke consisted of all the undetected carbon products such as amorphous and graphitic inert carbons including nonvolatile compounds which are detected with difficulty and analyzed by gas chromatography using FID and TCD detectors.

TG/DTA/mass-spectrometric Experiment on Mo/HZSM-5

The TG/DTA/mass-spectrometric study was performed using a TG/DTA/MASS System (MacScience Co., TG-DTA2020S) under a methane/He stream (flow rate; CH_4 = 15 ml/min and He 150 ml/min) and H_2/He (170 ml/min). 40–100 mg of Mo/HZSM-5 catalyst was loaded in a fused alumina boat and the evolved products such as H_2, CO, CO_2, C_2H_4, C_2H_6, C_6H_6, and $C_{10}H_8$ were continuously monitored with a TE-150 multiple channel mass spectrometer (MS-FISIONS) at m/e = 2, 28, 44, 26, 30, 78, and 128, respectively. The reaction temperature was raised from room temperature to 973 K with a ramping rate of 10 K/min and was kept at the specified value for 30 min. Before the reaction started, the catalyst was heated in a He stream at 873 K for 30 min and, in some cases, was further pretreated with H_2, methane, or ethane at 873 or 973 K for 30 min.

XAFS Measurements and SEM Study

The powdered and disk samples were charged under N_2 in an *in situ* XAFS cell with a Kapton film window (500 μm) to prevent exposure of the sample to air. Mo *K*-edge XAFS (X-ray absorption fine structure) measurements were conducted on the samples of Mo/HZSM-5 after impregnation, calcination at 873 K, and the reaction with methane at 873 K and 973 K at BL-10B at the Photon Factory of the National Laboratory for High Energy Physics (KEK-PF; Tsukuba, Japan). The energy and the current of the electron (or positron) were 2.5 GeV and 250 mA, respectively. An Si(311) channel cut monochromator was used. The XANES (X-ray absorption near edge structure) and EXAFS (extended X-ray absorption of the fine structure) spectra were analyzed by a computer program supplied by Technos Co. Ltd. [19]. The k^3 weighted EXAFS function was Fourier-transformed into *R*-space using the *k*-range from 3.5 to 18 $Å^{-1}$. The Hanning function used was $\delta = 0.5$ $Å^{-1}$. The phase shift was not corrected for the preliminary Fourier transformation. The inverse Fourier transform was calculated to obtain a filtered EXAFS function. The *R* range of an inverse Fourier transformation was taken from 1.09 to 3.31 Å. The Hanning function $\delta = 0.05$ $Å^{-1}$ was used as a window function. The fitting EXAFS parameters of the sample were determined for coordination number (C.N.) and interatomic distance *R*, for minimizing σ, and for correcting the threshold energy (ΔE_0). The backscattering amplitudes and phase shift functions of Mo–Mo, Mo–C, and Mo–O bonds were corrected using those of Mo foil (Mo–Mo), Mo_2C (Mo–Mo, Mo–C), and MoO_3 (Mo–Mo, Mo–O). The EXAFS parameters for discussion were fixed at the optimum value, and the residual factor *R* was calculated to offer the optimum values for the other parameters. The real value was estimated using a residual factor *R* which was less than half the optimum value. Each Mo/HZSM-5 sample with a Mo loading of 6 wt % before and after the carburization was studied by scanning-electron microscopy (SEM) (Hitachi-S 800).

IR Measurements of Pyridine Adsorption

Each powdered sample of 3 wt % Mo/HZSM-5 having different silica to alumina ratios in the range $SiO_2/Al_2O_3 = 20$–1900 was pressed into a self-supporting wafer (2.0 mm i.d., 15–18 mg/cm^2) at a pressure of 500 kg/cm^2. The wafer was mounted in an *in situ* IR cell equipped with a CaF_2 window. IR spectra were recorded using a step-scan Fourier Transform infrared spectrometer (Bio-rad FTS60A/896) with a resolution of 4 cm^{-1} and accumulation of 64 interferograms to improve signal/noise ratios in IR spectra. The IR measurements were conducted by the exposure of the disk of HZSM-5 after evacuation at 723 K for 2 h to the pyridine vapor of 1.2 kPa at 300 K.

RESULTS AND DISCUSSION

Reaction of Methane on Mo/HZSM-5 and Mo/FSM-16

The catalytic performance of 3% Mo/HZSM-5 in methane aromatization at 973 K and 1 atm pressure of methane was described in our previous study [17]. Hydrogen is usually produced in large amounts (H_2/benzene = 9–18 mol/mol) by the dehydrocondensation of methane. CO, CO_2, and H_2O are evolved at the initial stage of the reaction above 873 K due to the reduction of MoO_3 with methane, which converted molybdenum to lower valent state species or molybdenum carbide [9, 13, 14, 17]. The dependences of the methane conversion and the product formation rates on the reaction time on stream are presented in Fig. 1a. The conversion of methane (*ca.* 12%) usually decreases rapidly at the initial stage and moderately at the later stages of the reaction to 4% in 30 h of the time on stream. The suppression of the methane conversion may be attributed to the coke formation upon the admission of methane to the fresh Mo/HZSM-5 catalyst. This suggests that the deposited carbon becomes less reactive with time on stream, which also leads to the gradual deactivation of the catalyst. The major hydrocarbons produced on Mo/HZSM-5 consist of benzene, naphthalene, and toluene as aromatics, hydrocarbons, and C_2 products such as ethene and ethane. The total selectivity to gas-phase hydrocarbon products increases from 55% at the initial stage of the reaction to the constant value (70%) at the steady state of the reaction, while the selectivity of coke formation changes in a reverse way from 43 to 32%, as shown in Fig. 1b.

Figure 1c shows the composition of the gas-phase hydrocarbon products on the 3% Mo/HZSM-5 catalyst with the time on stream of the methane reaction. At the initial stage of the reaction, C_2 species, benzene, toluene, and naphthalene are produced with the yields of 4, 50, and 45%, respectively, on the carbon basis. After 24 h, the naphthalene content in the hydrocarbon products decreases from 45 to 12%, while the percentage of C_2 and benzene increases to about 20 and 68%, respectively, at the expense of the decrease in the naphthalene yield. This may suggest that naphthalene is apparently produced consecutively from C_2 species and benzene, as proposed by the consecutive mechanism as depicted in scheme 1, as it has been previously reported [8–10, 13, 17] (Scheme 1).

We collected all the aromatic products in the effluent gas which were condensed in the ethanol–dry ice trap. The reaction products were analyzed by the online MS-GS with a capillary column (OV-1, 25 m) up to 553 K and the MALDI-TOF time-of-flight reflection mass spectrometer VOYAGER (*m/e* = 2500; PerSeptive Biosystems Co.). Figure 2 shows a list of aromatic compounds such as benzene and naphthalene as the major products including other polycondensed aromatics such as anthracene, pyrene, tetracene, and their methyl-substituted compounds. The latter polycondensed aromatic compounds are analyzed with difficulty by the on-

line GC system due to their high boiling point and strong adsorption on the Mo/HZSM-5 catalysts even at temperatures higher than 873 K. The molar fractions of methyl-substituted products such as toluene and methylnaphthalene are kept constant at 3–5% during the reaction process. Bulky aromatic compounds other than benzene and naphthalene, are marginally obtained on the Mo/HZSM-5 catalyst partly because of the higher activity in hydrogenolysis and molecular shape selectivity due to the limited size of the micropores of HZSM-5. On the other hand, it is of interest to find that the catalytic performance of Mo supported on FSM-16 having larger pores of 2.7 nm is characterized by the lower yield of benzene and high contribution of polycondensed aromatic compounds and coke in the methane conversion (Table 1). It was found that, although the initial conversion of methane was very high, the 3 wt % Mo/FSM-16 was drastically deactivated for a few hours, in comparison with Mo/HZSM-5. 3 wt % Mo/FSM-16, regardless of its Si/Al ratios of 15–320, yielded hydrocarbons such as benzene and C_2-hydrocarbons in less than 20% selectivity owing to the enormous coke formation (with the selectivity over 80%), similar to the 3% Mo supported on amorphous silica. This suggests that the microporous channels of HZSM-5 (10.6 nm) are effective for preferential formation of smaller aromatics such as benzene and naphthalene and preventing the formation of graphitic coke and high-condensed aromatics in the methane conversion.

Promotion of Dehydroaromatization of Methane by CO Addition

The addition of CO to methane feed gas exerts a significant effect on the catalytic performance of Mo/HZSM-5 shown in Fig. 3 and Co-modified Mo/HZSM-5 presented in Fig. 4 for the aromatization reaction, promotes the benzene formation, and improves the catalyst stability. When pure CH_4 was used as the feed gas, the methane conversion and benzene formation rate were sighificantly decreased during 24 h of the reaction time on stream, as shown in Figs. 3 and 4. With the addition of CO in the feed gas, the methane conversion drop was substantially moderated regardless of the partial pressure of CO (from 1.7 to 12.3%). After attaining an increase in the benzene formation at the early stage of methane conversion with CO, the benzene formation rate was almost constant during the prolonged reaction up to more than 24 h. It is noteworthy that, in the steady state, the amount of CO is virtually constant before and after the reaction in all the cases of CO addition. The results imply that CO is possibly regenerated due to the efficient removal of surface carbon deposits with the active oxygen species which is derived from CO dissociation as shown in scheme 2 [19, 20].

By changing the amount of CO added to the 1 atm methane flow at 973 K, the Mo/HZSM-5 and Co-modified Mo/HZSM-5 catalysts exhibit appreciable promo-

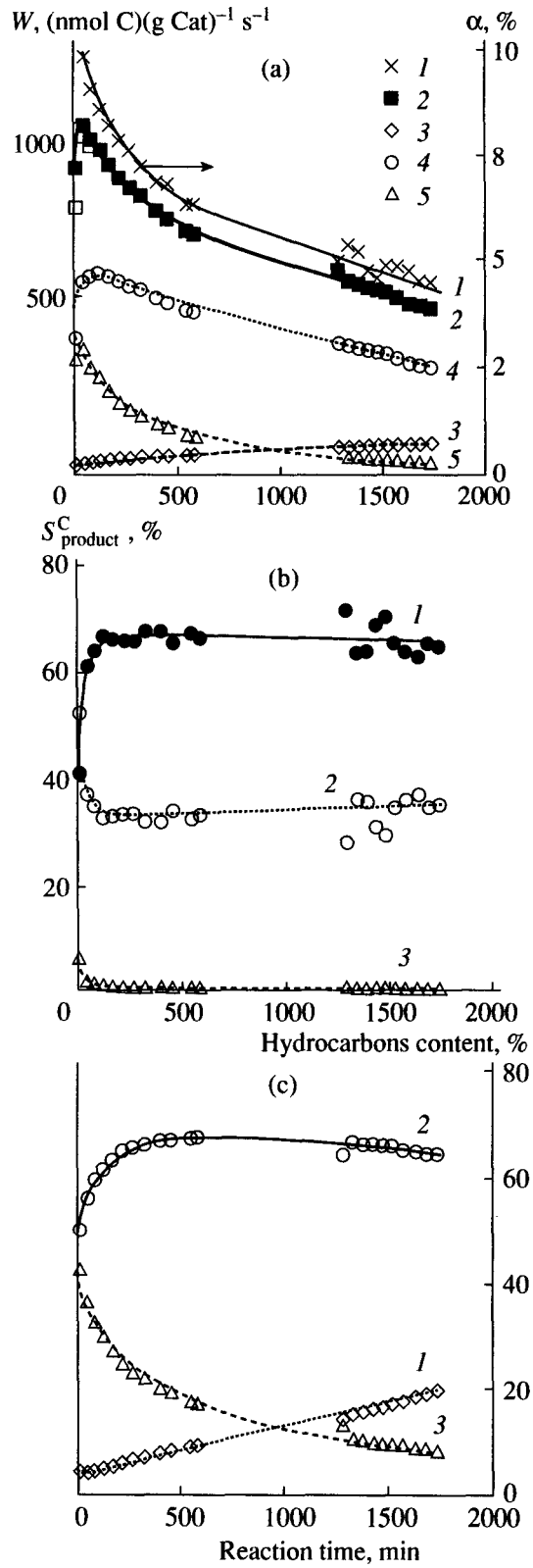

Fig. 1. Catalytic performances in the methane conversion at 973 K on 3 wt % Mo/HZSM-5; (a) methane conversion (%) and rates of product formation for benzene, naphthalene, and C_2 hydrocarbons on the carbon base ((nmol s^{-1} (g Cat)$^{-1}$), (b) selectivities of hydrocarbons and coke vs. time on stream, and (c) product composition (%) on carbon base for hydrocarbon products vs. the time-on-stream (min).

Mechanism of the dehydrocondensation of methane to aromatic products such as benzene and naphthalene via the surface hydrocarbon species on Mo/HZSM-5 catalysts

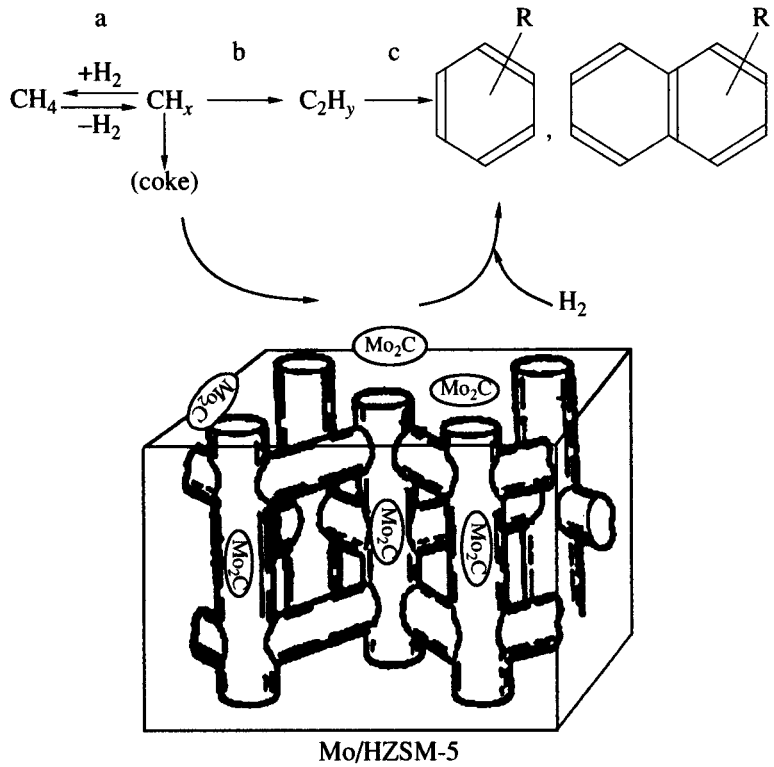

Scheme 1.

tion of catalytic activities in the benzene formation at 973 K and 1 atm of methane (120–150 nmol/g-cat/s) at high selectivity (75–85% at 10–13% CH_4 conversion) for the prolonged time on stream as shown in Fig. 4. The rate of benzene formation decreases moderately, but the rates remain high and the selectivity to coke is low (less than 10%) for 100 h. By varying the concentration (1.8–12.0%) of CO in the methane feed, we demonstrated that the similar promotion regardless of the CO concentration was attained at 973 K on the 3%

Table 1. Catalytic performances of 3 wt % loading Mo catalysts (0.3 g) using various supports for CH_4 aromatization reaction at 973 K; P_{CH_4} = 1 atm, flow rate = 7.6 ml/min

Catalyst*	Time on stream, (min)	α_{CH_4}, conversion %	Formation rate of the products, W (nmol C)(g Cat)$^{-1}$ s^{-1}										
			H_2	CO	CO_2	C_2H_4	C_2H_6	C_3H_6	C_6H_6	C_7H_8	C_{8-9}	$C_{10}H_8$	C_{11-12}
3%Mo/HZSM-5 (39.5)	40	9.57	2879	38.9	0.0	12.72	9.74	0.0	113.5	6.19	0.34	25.42	0.0
3%Mo/HZSM-5 (23.8)	40	9.63	2940	78.8	0.0	7.08	8.89	0.23	82.29	4.30	0.0	23.12	0.32
	108	7.86	2332	24.6	0.0	15.00	10.12	0.62	99.42	5.92	0.69	26.70	0.45
PMoW/HZSM-5 (39.5)	40	10.28	2941	42.9	0.0	12.39	9.72	0.39	106.5	5.58	0.30	36.24	0.37
PVMo/HZSM-5 (39.5)	40	5.08	1327	58.8	0.0	19.03	9.00	1.07	43.21	4.51	0.0	9.05	0.0
25%Mo/FSM-16 (4.7 nm)	40	1.42	509	41.5	0.0	3.22	1.24	0.0	2.07	1.50	0.0	0.67	0.0
3%Mo/H-Mord (N5)**	40	6.94	2361	101.2	0.0	14.31	8.13	0.43	12.58	0.98	0.0	34.99	2.21
6%Mo/C**	40	2.21	937	10.0	0.0	4.34	1.71	0.0	1.39	0.17	0.0	1.07	0.0
3%Mo/FSM-16 (20)	40	10.32	4262	73.7	0.0	4.77	4.66	0.24	9.21	0.64	0.0	10.00	0.0
	153	5.19	1919	28.8	0.0	6.97	2.88	0.27	18.42	1.39	0.0	38.48	2.84
3%Mo/FSM-16**	40	15.10	7398	112.6	0.0	3.48	4.91	0.0	2.50	0.29	0.0	2.86	0.0
(2.7 nm)	158	7.07	2665	44.0	0.0	6.55	4.20	0.23	17.30	1.24	0.0	25.59	1.00

* The SiO_2/Al_2O_3 ratio in the zeolite or a pore size is given in brackets.

** The formation of $C_{10}H_8$ and C_{11-12} is not accurate.

Mo/HZSM-5 catalyst. This promotion significantly stabilizes the formation rates of the hydrocarbons, namely, C_2-hydrocarbons, benzene, and naphthalene, at the time on stream over 30 h when compared with the rates obtained using pure methane. It is obvious that the addition of CO to methane resulted in the enhancement of the naphthalene formation, while suppression of the yield of C_2 hydrocarbons was possibly due to the reduction of coke poisoning the catalyst. Although the product selectivities and promotion of the catalyst stability were substantially affected by adding CO to the methane feed, it was of interest to find that CO added in the conversion of methane was apparently not consumed. In fact, during the conversion of methane with CO, the concentrations of CO in the gas phase of the reaction are kept unchanged and close to that in the methane feed in the due course of the reaction.

Effect of CO_2 Addition on the Methane Conversion on Mo/HZSM-5

The 3 wt % Mo/HZSM-5 catalyst for the methane dehydrocondensation at 973 K was also improved by adding 1.6% CO_2 to the methane feed gas, as shown in Fig. 5. The addition of 1.6% CO_2 resulted in a higher methane conversion and hydrogen formation rate at the early stage of the reaction, possibly owing to the reforming reaction ($CO_2 + CH_4 = 2CO + 2H_2$). Both the methane conversion and the benzene yield were fairly stable upon addition of 1.6% CO_2. A similar effect was revealed after addition of 4–12% CO to methane on the Mo/HZSM-5 catalyst as shown in Figs. 3 and 4. However, the methane conversion was greatly suppressed by increasing the CO_2 concentration higher than 2%. In contrast to CO addition, it was found that an excess of CO_2 (>2%) in the methane feed gas largely inhibited the formation of aromatic products such as benzene and naphthalene in spite of significant evolution of CO and hydrogen due to the reforming reaction. Figure 5 shows that the addition of 12% CO_2 to the methane feed resulted in a complete inhibition of the formation of aromatic products such as benzene and naphthalene. A small amount of C_2 hydrocarbons was only produced in the conversion of methane with 12% CO_2 at 973 K on Mo/HZSM-5. These data are is in agreement with the marked suppression of benzene formation by the pulse addition of 10% CO_2 in the reaction of methane on Mo/ZSM-5, which has been reported previously by Lunsford *et al.* [12].

The formed CO may exert a similar promotion of product formation and improvement of the catalytic stability owing to efficient suppression of coke deposition on the catalysts. No appreciable differences in product selectivities for benzene using either pure methane or methane plus CO or CO_2 were found on Mo/HZSM-5, as is shown in Figs. 3 and 5. The results similar to those observed after the addition of 12% CO_2 were obtained upon the addition of a few percents of O_2 to the methane feed at 973 K, which resulted in the

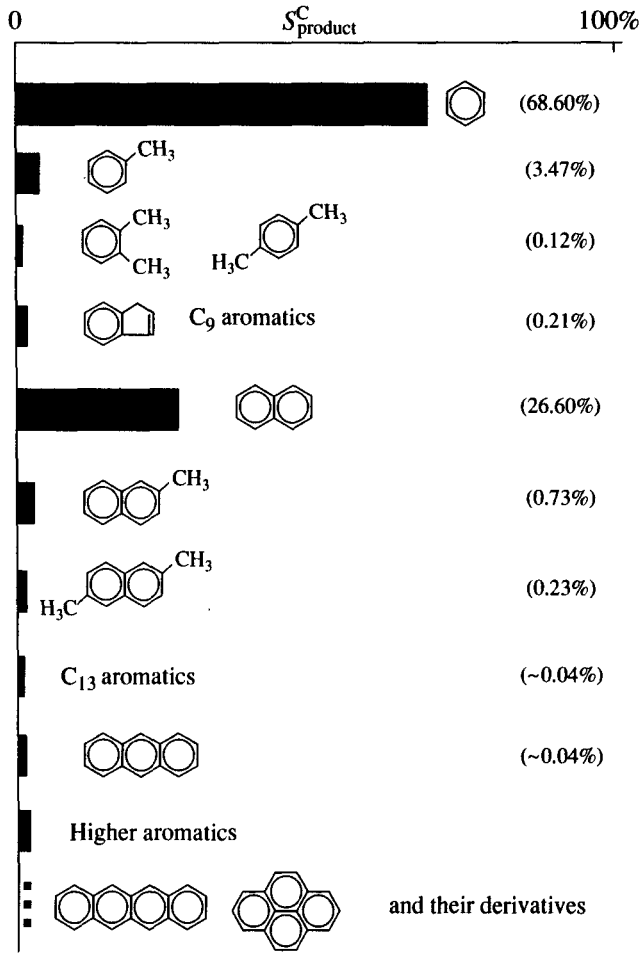

Fig. 2. Distribution (on the carbon basis) of the aromatic compounds formed in an atmospheric methane dehydrocondensation on 3 wt % loading Mo/HZSM-5 at 973 K for 4 h.

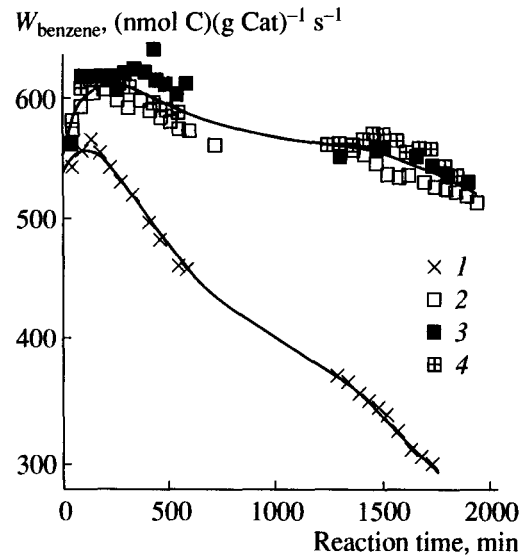

Fig. 3. Effect of CO addition to methane feed on the rate of benzene formation (nmol C)(g Cat)$^{-1}$ s^{-1} on the carbon basic for Mo/HZSM-5 and varied CO concentrations vs. time on stream (min).

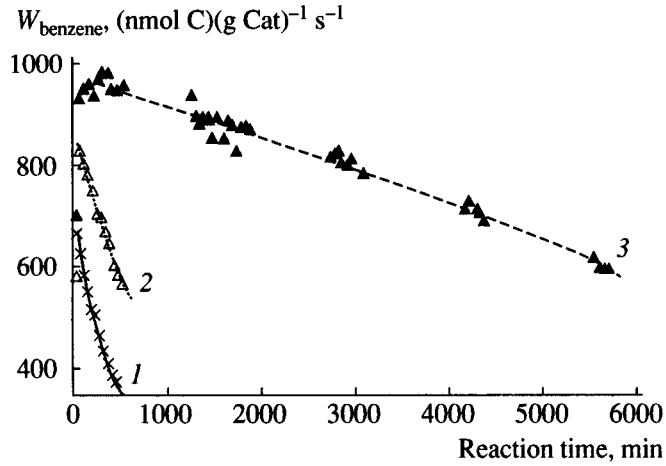

Fig. 4. Effect of CO addition to methane feed on the formation rate of benzene of the carbon basis (nmol C)(g Cat)$^{-1}$ s^{-1} on 1 wt % Co and 3 wt % Mo/HZSM-5 at 973 K vs. time on stream.

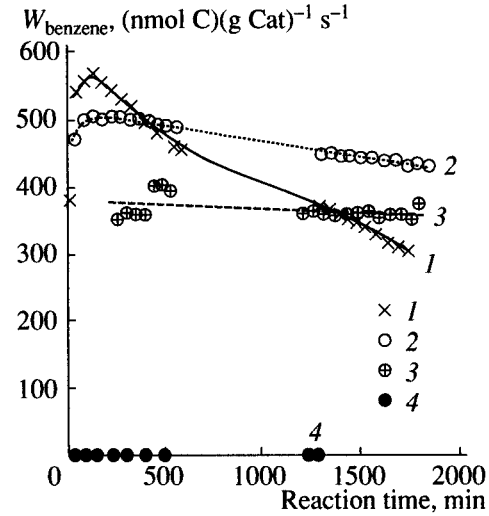

Fig. 5. Effect of CO_2 addition to the methane feed on the formation rate (nmol C)(g Cat)$^{-1}$ s^{-1} on the carbon basis (CO_2 concentrations of 1.6, 4.1, and 12%) vs. time on stream (min).

complete inhibition of the formation of benzene on 3% Mo/HZSM-5.

The different effects of CO and CO_2 on the methane aromatization may be associated with their different chemical reactivities: CO dissociates at 973 K to form [O] and [C], which reacts with methane (or hydrogen) to form the common active CH_x and C_2H_y species. A C_2 intermediate such as ethylene is converted to aromatics such as benzene and naphthalene on Mo/HZSM-5. On the other hand, the dissociative [O] species from CO and CO_2 may react with surface coke to regenerate CO. CO_2 is more active to react with surface carbon which is derived from the methane conversion, yielding two moles of CO. CO_2 addition to methane promotes the catalyst stability similarly to CO. Such an effective consumption of surface carbon and oxidation of Mo sites on the HZSM-5 support by the excess amount of CO_2 causes the marked suppression of methane aromatization towards benzene and naphthalene. Similar to the previous discussion about the poisoning effect of the coke, there is an analogous explanation that the catalytic formation of aromatics such as benzene requires a large ensemble (surface concentration) of active CH_x species on the Mo sites in the vicinity of the HZSM-5 support [15, 20].

As shown in Fig. 6, it was demonstrated by the temperature-programmed oxidation (TPO) experiments (ramping temperature rate, 2 K/min; air flow rate, 20 ml/min) that the amount of coke deposition on the catalyst surface was greatly reduced by adding various amounts of CO or CO_2 to the methane feed gas. An increase in the CO concentration from 1.8% to 12.0% in the methane flow resulted in a marked suppression of the total coke formation on the catalyst surface, particularly the irreversible or inert coke which was oxidized to CO_2 at the higher temperature above 773 K in the TPO experiment. An increase in the CO_2 partial pressure (1.6 to 4.1%) in the methane feed gas effectively decreased the coke formation on the catalyst to a much lower level compared with the effect caused by CO.

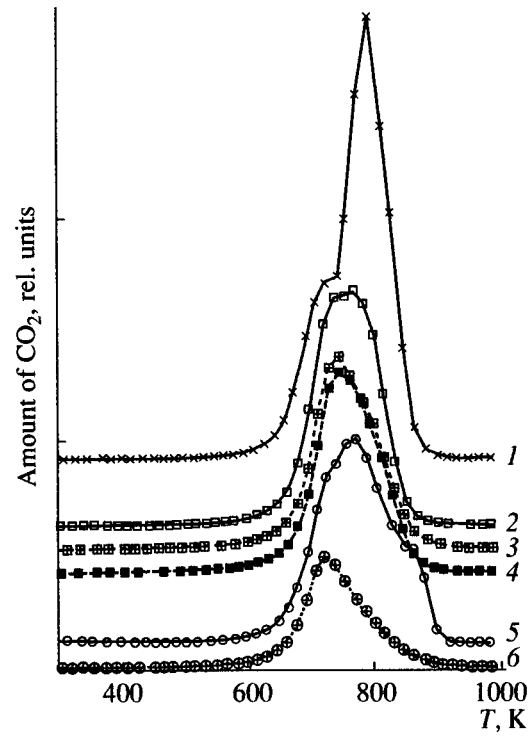

Fig. 6. TPO patterns of the 3 wt % Mo/HZSM-5 catalyst after a methane aromatization reaction running for 6 at 973 K and a pressure of 1 atm with different amounts of CO or CO_2 added to the methane feed gas. (*1*) only CH_4; (*2, 3, 4*) 1.8, 4.0, and 12% CO added; (*5, 6*) 1.6 and 4.1% CO_2 added. (TPO experiments were carried out using 300 mg of the catalyst at an air flow rate of 20 ml/min and a heating rate of 2 K/min).

Mechanism for the promotion of CO/CO_2 addition to a methane feed to improve the catalyst stability and to reduce the coke formation on Mo/HZSM-5 catalysts

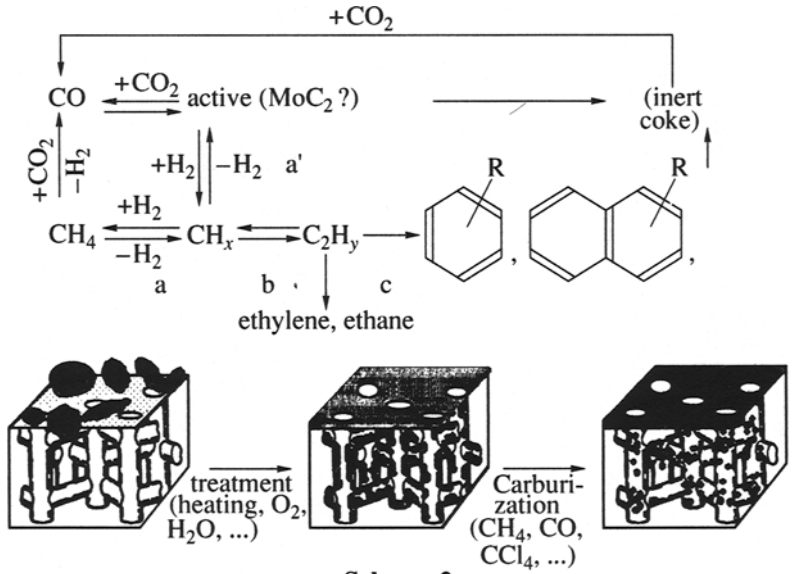

Scheme 2.

This may be related to the higher activity of the dissociated oxygen in the reaction with the surface carbon to form CO ($CO_2 + C \longrightarrow 2CO$) as shown in Scheme 2.

To understand the role of CO in the methane aromatization reaction, the $^{13}CO + CH_4$ reaction was conducted in a closed circulating reaction system. The starting composition of the reactant mixture is 8% ^{13}CO + 92% CH_4 with a total pressure around 220 torr. Even after 5 min of the closed circulating reaction at 973 K, ^{13}C atoms involved in methane ($^{13}CH_4$) the value of 8%. The isotopic abundance of ^{13}C incorporated in the benzene molecule was detected by GC-MS analysis as the random distribution ($^{13}CC_5H_6$—47.6%, $^{13}C_2C_4H_6$—36.7%, $^{13}C_3C_3H_6$—13.0%, $^{13}C_4C_2H_6$—2.4%, $^{13}C_5CH_6$—0.3%) regardless of the reaction time of methane on Mo/HZSM-5. These results suggest that the carbon derived from CO dissociation is efficiently incorporated in the benzene formation and the isotopic scrambling reaction between ^{13}CO and $^{12}CH_4$ proceeds rapidly under the reaction conditions at 973 K, as shown in Fig. 7. Based on the above results, we suggest the mechanism of the unique role of CO in the methane aromatization reaction which is reduced to stabilization of the catalyst performance and promotion of the benzene formation as shown in Scheme 2. First, CO dissociates on the Mo sites (Mo_2C) to form the active carbon species CH_x and C_2 through reactions (a') and (b) followed with their oligomerization to form higher hydrocarbons such as benzene and naphthalene in reaction (c) on the catalyst. The dissociated oxygen species [O] from CO may react with the surface inert carbon species (coke) to regenerate CO, resulting in the suppression of the coke formation on the catalyst through reaction: $CO \longrightarrow [C] + [O]$, $CO_2 \longrightarrow CO + [O]$, [O] + coke $\longrightarrow$ CO.

Influence of the Silica to Alumina Ratio in HZSM-5 on the Brönsted Acidity and Methane Aromatization Activity on Mo/HZSM-5

A series of 3 wt % Mo/HZSM-5 catalysts was prepared using different SiO_2/Al_2O_3 ratios. The perfor-

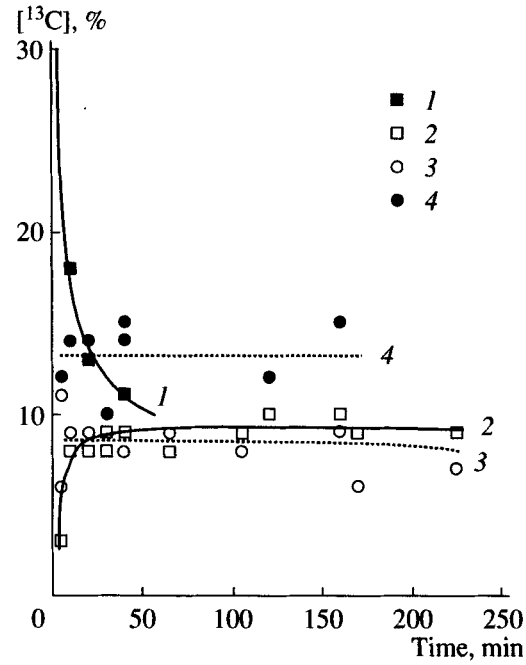

Fig. 7. Average abundance (%) of ^{13}C atoms in the methane, CO, ethene, and benzene molecules formed in the reaction with a mixture gas of methane (92%) and ^{13}CO (8%) [total pressure of 220 torr] on the 3 wt % Mo/HZSM-5 catalyst at 973 K in a closed circulating reactor vs. exposure time (min).

mances in the methane conversion at 973 K have been studied on the catalysts in conjunction with the SiO_2/Al_2O_3 ratio (20–1900) of HZSM-5 as shown in Fig. 8. It is of interest to find that the rates of benzene formation on the Mo/HZSM-5 catalysts substantially depend on the SiO_2/Al_2O_3 ratios of the HZSM-5 used, showing the maximum activities of methane aromatization for the HZSM-5 supports having a SiO_2/Al_2O_3 ratio of 30–45. By contrast, the Mo/HZSM-5 having lower and higher SiO_2/Al_2O_3 ratios than the optimum values of 30–45 exhibited activities for the benzene formation that were lower by one or two orders of magnitude and serious coke formation as compared to the Mo/HZSM-5 catalyst having a SiO_2/Al_2O_3 ratio of 40. The Brönsted and Lewis acidity of the samples have been determined by pyridine adsorption using FT-IR spectroscopy. Figure 9 shows the IR spectra of pyridine adsorbed on 3 wt % Mo/HZSM-5 catalysts with different SiO_2/Al_2O_3 ratios. Upon pyridine adsorption at room temperature and outgassing at 423 K, absorption bands associated with the chemisorbed pyridine were observed at 1547, 1491, and 1454 cm^{-1}. According to the previous reports on the IR studies of pyridine chemisorption [21, 23], the pyridine band at 1547 cm^{-1} is assigned to pyridinium ions, and the band at 1454 cm^{-1}, to Lewis acid-coordinated pyridine. The band at 1491 cm^{-1} consists of two bands due to the Brönsted and Lewis sites. All the spectra were normalized using the peak intensities of the ZSM-5 support at around 1873 cm^{-1} as a standard, and the intensities of bands at 1547 cm^{-1} for Brönsted acid and 1454 cm^{-1} for Lewis acid sites were used for probing of acidity of the Mo/HZSM-5 catalysts having different SiO_2/Al_2O_3 ratios. By contrast, the band around 1440 cm^{-1} assigned to Lewis acid sites somewhat increased on Mo/HZSM-5 after calcination at 773 K and even after the methane aromatization reaction at 973 K. There is a correlation between the Lewis acidity and the lattice substituted metal ions such as Al^{3+} and higher valent Mo species such as Mo^{6+}.

As shown in Fig. 8, the variations of Brönsted and Lewis acidity on Mo/HZSM-5 and those of the benzene formation rates and coke selectivities in the methane aromatization on Mo/HZSM-5 catalysts are illustrated as the function of the SiO_2/Al_2O_3 ratios of the HZSM-5 supports used. The Brönsted acidity of HZSM-5 showed a sharp maximum for the HZSM-5 having the SiO_2/Al_2O_3 ratio of 39.5, which is identical to that of benzene formation rates. Nevertheless, there is no particular relationship between the benzene production and the Lewis acidity of Mo/HZSM-5 which monotonously decreases with an increase in the SiO_2/Al_2O_3 ratio of the used HZSM-5. According to the close correlation between the Brönsted acidity of the Mo/HZSM-5 catalysts and benzene formation rates in the methane aromatization reaction, it is reasonable to suggest than the aromatic products such as benzene are most probably promoted by the Brönsted acid sites rather than by the Lewis acid sites of the ZSM-5 support. Moreover, as shown in Fig. 8, it was demonstrated

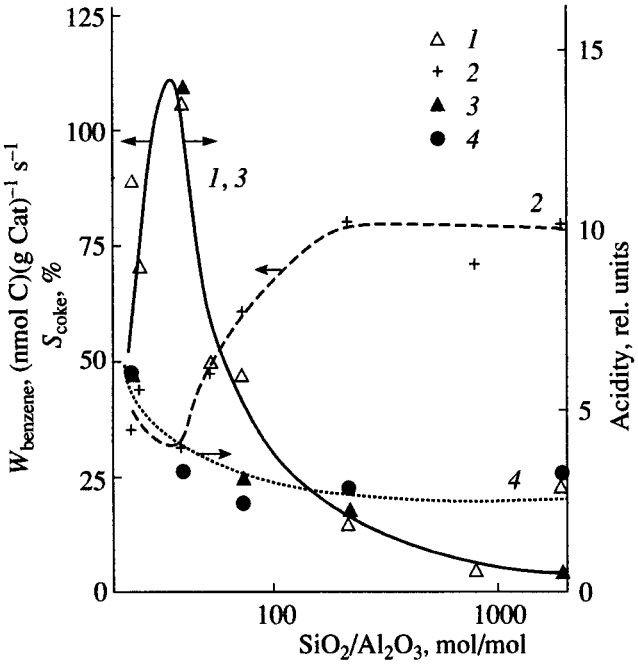

Fig. 8. Benzene formation rates (nmol C)(g Cat)$^{-1}$ s^{-1}, coke selectivity (%) in the methane reaction at 973 K, and Brönsted and Lewis acidities deduced by the IR study of pyridine adsorption on the 3 wt % Mo/HZSM-5 upon the SiO_2/Al_2O_3 ratios of the HZSM-5 used.

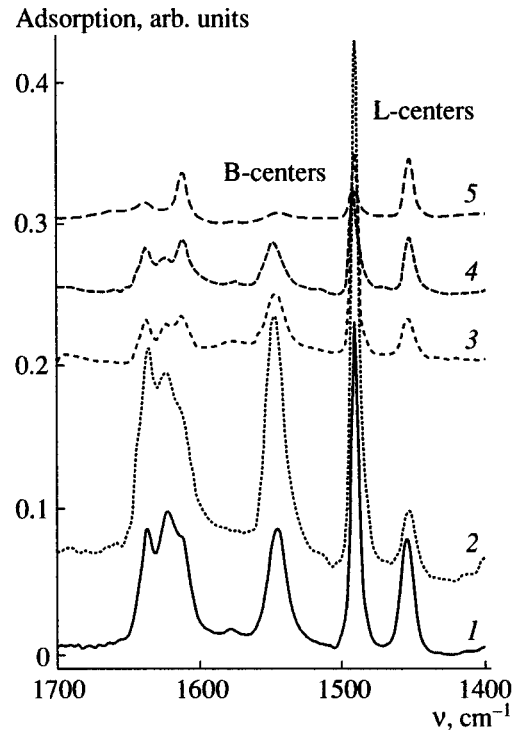

Fig. 9. IR spectra of adsorbed pyridine on 3% Mo/HZSM-5 with various SiO_2/Al_2O_3 ratios of supporting HZSM-5: (*1*) 23.8, (*2*) 39.5, (*3*) 73.4, (*4*) 213, and (*5*) 1900.

that the coke selectivities in the methane conversion on Mo/HZSM-5 are minimized (less than 30%) for the HZSM-5 having the optimum SiO_2/Al_2O_3 ratio of 39.5, whereas the coke forms seriously up to over 85% on the HZSM-5 catalysts with the lower or higher SiO_2/Al_2O_3 ratio deviated from 35–45. The higher Brönsted acidity of the HZSM-5 supports may bifunctionally promote not only the methane activation ($CH_4 \longrightarrow CH_x + \frac{4-x}{2}H_2$) on the Mo carbide sites of Mo/HZSM-5 catalysts, but also the further oligomerization of the dissociative CH_x surface species towards the primary products (such as ethene) which are effectively converted into benzene and naphthalene on the Mo/HZSM-5 catalysts.

Mo Carbide Formation on Mo/HZSM-5 Characterized by EXAFS/SEM and TG/DTA/MS

The X-ray diffraction patterns of calcined or carburized supported samples (Mo/HZSM-5) with a loading of up to 6% showed no peaks corresponding to molybdenum oxide or molybdenum carbide because of the high dispersion of both Mo crystallites on the HZSM-5 supports as suggested previously [12, 13, 17]. The unsupported Mo_2C sample showed peaks corresponding to Mo_2C of the hexagonal close-packed crystal structure with normal lattice parameters $a = 2.99$ Å and $c = 4.72$ Å. To characterize the active structure of the Mo/HZSM-5 catalyst of methane aromatization, the Mo *K*-edge XAFS studies have been conducted using the 10 B line at the Photon Factory of the National Laboratory for High Energy Physics (KEK-PF; Tsukuba, Japan). The corresponding Fourier-transform functions are shown in Fig. 10. Three dominant peaks in each spectrum represent the Mo–C distance in Mo_2C (1.58 Å), the Mo–Mo distance in Mo_2C (2.62 Å), and the Mo–Mo distance in metallic Mo (2.38 Å) as the reference samples, respectively. These distances should be corrected for phase shifts of 0.34 Å for Mo–Mo and 0.5 Å for Mo–C distances. After the calcination of the sample containing 6 wt % Mo sample, $(NH_4)_6Mo_7O_{24}$/HZSM-5, at 973 K prior to the methane reaction, the Mo *K* edge Fourier-transform functions showed that the spectrum of the calcined sample (Fig. 10, spectrum *2*) consists of an intense peak at 1.42 Å, possibly due to the Mo–O bond of highly dispersed Mo oxide species similar to $NaMo_4$ and $[Mo(=O)_4]$ in NaY as reported by Ozin [25]. The FT function spectrum (Fig. 10, spectrum *2*) is different from that of the MoO_3 crystal (Fig. 10, spectrum *1*). The EXAFS data suggest that Mo oxide species in the calcined sample of Mo/HZSM-5 are highly dispersed in the internal channels of HZSM-5. The FT function of the sample reacted with methane at 973 K for 1 h (Fig. 10, spectrum *3*) and at 973 K for 24 h (Fig. 10, spectrum *4*) showed peaks at the same positions as those for the Mo_2C reference (Fig. 10, spectrum *5*). The spectra of two samples (Figs. 10, spectra *3* and *4*) are identical in every detail except for the peak at 2.23 Å, possibly due to molybdenum oxycarbide. The structural data abstracted from the curve-fitting of the FT function for the samples of Mo/HZSM-5 after the carburization with methane at 973 K are listed in Table 2. The results suggest that the impregnated sam-

Table 2. EXAFS parameters for the Mo/HZSM-5 in the methane reaction at 973 K in comparison with those of Mo foile and Mo_2C

Samples	Mo–Mo			Mo–O(C)		
	C.N.	*R*, Å	σ*	C.N.	*R*, Å	σ*
3 wt % Mo/HZSM-5, 973 K, 1 h	2.1	2.97	0.084	0.8	2.10	0.047
3 wt % Mo/HZSM-5, 973 K, 24 h	2.3	2.98	0.087	0.9	2.14	0.055
6 wt % Mo/HZSM-5, 973 K, 4 h	2.5	2.96	0.095	0.6	2.11	0.028
Mo foil	8	2.72	0.064	–	–	–
MoC_2	12	2.97	0.071	3	2.09	0.047

* σ Debye–Waller factor.

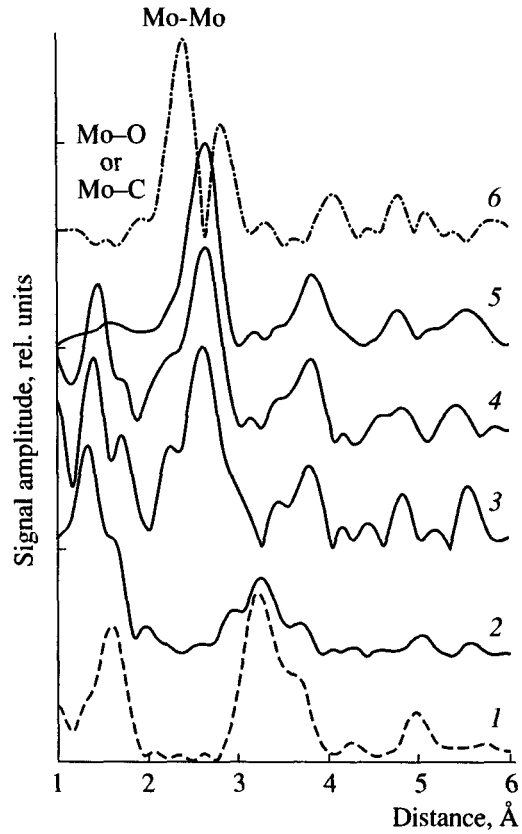

Fig. 10. Mo *K* edge EXAFS Fourier-transform function spectra of (*1*) a MoO_3 crystal; (*2*) 6 wt % Mo/HZSM-5 after calcination at 873 K for 2 h; (*3*) after treatment of (*2*) with methane at 973 K for 1 h; (*4*) after treatment of (*2*) with methane at 973 K for 24 h; (*5*) Mo_2C powder; and (*6*) a Mo foil as the reference.

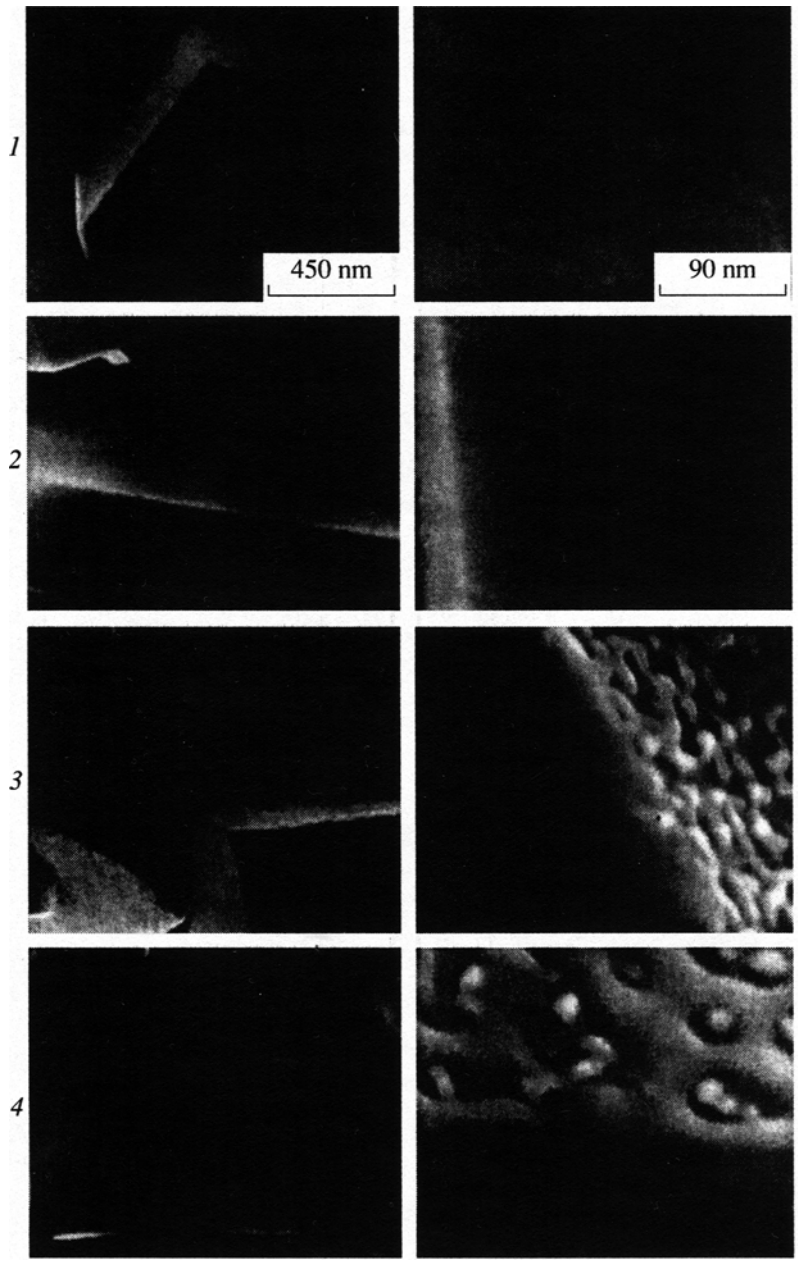

Fig. 11. SEM picture of Mo/HZSM-5 crystals (1.8 μm) before and after the precarburization and methane conversion at 973 K. (*1*) $C_{10}H_8$ (*m/e* = 128), (*2*) C_2H_6 (*m/e* = 30), (*3*) H_2 (*m/e* = 2), (*4*) C_2H_4 (*m/e* = 26), (*5*) CO (*m/e* = 28), (*6*) C_6H_6 (*m/e* = 78).

ple of 3 wt % Mo/HZSM-5 and 6 wt % Mo/HZSM-5 after the calcination at 873 K consists of an isolated Mo oxide, which might be highly dispersed in the internal channels of HZSM-5 (6 Å diameter). After the reaction with methane at 973 K for 1 and 24 h, the Mo oxide species is converted with methane to a Mo_2C cluster (Mo–Mo; coordination number (CN) = 2.1–2.5; R = 2.96–9.28 Å; Mo–C; CN = 0.8–0.9, R = 2.12–2.14 Å) in comparison with those of Mo_2C reference (Mo–Mo; CN = 12, R = 2.79 Å; Mo–C; CN = 3, R = 2.10 Å) [23, 24]. The FT function spectra of Mo/HZSM-5 retained a partial contribution of Mo oxide in precarburization and even after prolonged conversion with methane at 973 K as indicated in Fig. 10, specrta *2–4*. These results imply that the Mo oxide species dispersed in the HZSM-5 framework may migrate at the external surface of HZSM-5 and be converted with methane to Mo carbide, which is spread on the support surface and is active in methane aromatization at 973 K. It is of interest to find by the SEM observation (Fig. 11) that nanostructure Mo carbide particles (2 nm) are uniformly dispersed on the HZSM-5 crystal surface after the precarburization with methane at 873–973 K for 1 h on 6% Mo/HZSM-5. The Mo carbide particles remained

unchanged during the methane conversion toward benzene at 973 K for 4 h without any formation of coke and carbon fibers.

The temperature-programmed reaction (TPR) with methane was conducted on 3 wt % Mo/HZSM-5 using TG/DTA/MS by flowing methane while heating from 300 to 973 K. As shown in Fig. 12, the evolution of CO (m/e = 28) and H_2 (m/e = 2) occurred at 923–973 K, when molybdenum oxide is converted to Mo_2C. This initiates the methane conversion to C_2 products, ethene (m/e = 26), ethane (m/e = 30), benzene (m/e = 78), and naphthalene (m/e = 128) accompanied with hydrogen (m/e = 2) evolution. On the other hand, the DTA pattern in a methane stream on Mo/HZSM-5 shows a distinct endothermic peak at 955 K due to the Mo carbide formation, whereas no particular peak arises in the hydrogen flow. The TG pattern in a methane flow offers a sharp weight loss at 957 K due to the Mo carbide formation, accompanied by a gradual weight increase above 960 K, possibly owing to the coke formation on Mo/HZSM-5 in the reaction with methane. These data of EXAFS and TG/DTA/MS studies indicate that Mo oxide on HZSM-5 is carburized with methane at 923–963 K to form Mo_2C clusters with high dispersion, which initiates the methane aromatization to benzene and C_2 hydocarbons at 973 K, as indicated in scheme 2.

It is conceivable that the HZSM-5 supports having proper acidities catalyze a coupling of carbon species CH_x to ethylene which is oligomerized to benzene and naphthalene by analogy with the catalytic aromatization of alkanes at 523–623 K, referred to as a Mobil process [26]. The evidence of synergetic promotion in the physical mixture of Mo/SiO_2 + HZSM-5 and Mo_2C + HZSM-5 implies that the active carbon species may migrate to HZSM-5 in the vicinity of Mo carbide sites via the formation of C_2 products such as acetylene, ethene, and ethane, which are converted to aromatics such as benzene and naphthalene. In this sense, the bifunctional role of Mo carbide and HZSM-5 for the methane aromatization has a close analogy with the synergetic promotion of Pt/alumina catalysts for the alkane reforming process consisting of the dehydrogenation of alkanes to olefins catalyzed on Pt sites, which migrate to the acidic alumina support, resulting in the dehydrocyclization to benzene derivatives. In addition, Boudart *et al.* [24] reported previously that Mo carbide is catalytically active for the dehydrogenation towards olefins and hydrogenolysis of alkanes, similar to the typical noble metals such as Pt and Ir.

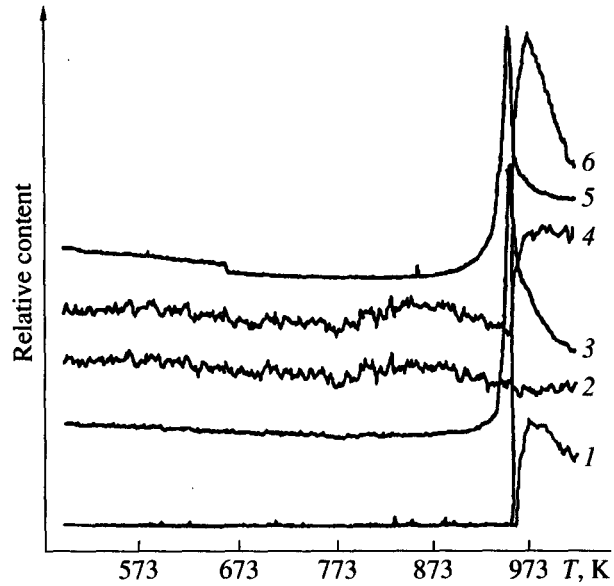

Fig. 12. TPR spectra for the product formation evolved in the reaction with methane on 3 wt % Mo/HZSM-5 (SiO_2/Al_2O_3 ratio of 39.5) by heating from 300 to 973 K and holding at 973 K for 30 min. Flow rate: CH_4/He = 15/150 (ml/min); heating rate of 5 K/min.

CONCLUSION

The present work may be summarized by the following conclusions:

(1) Catalytic dehydroaromatization of methane with CO and/or CO_2 proceeds at 973 K under an atmospheric pressure of methane on Mo/HZSM-5 and Fe/Co modified Mo/HZSM-5 towards aromatic products such as benzene and naphthalene with high yields and stable selectivities (above 85%) and minimizing the coke formation (less than 10%) for the prolonged time on stream.

(2) The marked promotion by CO and/or CO_2 addition to methane is associated with effective suppression of the polycondensation of aromatics and reduction of the coke formation with active oxygen derived from CO and CO_2 on the Mo/HZSM-5 catalysts.

(3) Bifunctional catalysis of Mo/HZSM-5 is discussed using the mechanism involving methane activation on Mo carbide sites to form CH_x and C_2 species, which may migrate at the interface of ZSM-5 having the optimum acidity for the dehydrocyclization to benzene and naphthalene.

(4) The TG/DTA/MS and EXAFS studies reveal that the Mo oxide supported on HZSM-5 is endothermically converted at 955 K with methane with evolution of H_2 and CO to molybdenum carbide Mo_2C, which initiates the methane conversion around 960 K, yielding benzene, naphthalene, and C_2 hydrocarbons.

ACKNOWLEDGMENTS

This work was supported by the Proposal-Based New Industry Creative Type Technology P&D Promotion Program from the New Energy and Industrial Technology Development Organization (NEDO) of Japan. The authors thank Dr. Inagaki and Dr. Fukushima, Tokyota Central Research Laboratory, for their gifts of the mesoporous materials of FSM-16 and helpful discussion on the bifunctional role of the supports for the methane dehydroaromatization on the Mo catalysts.

REFERENCES

1. Fox, J.M., *Catal. Rev.-Sci. Eng.*, 1993, vol. 35, no. 2, p. 169.
2. Brown, M.J. and Parkyns, N.D., *Catal. Today*, 1991, vol. 8, no. 1, p. 305.
3. Kuo, J.C.W., Kresge, C.T., and Palermo, R.E., *Catal. Today*, 1989, vol. 4, p. 463.
4. Krylov, O.V., *Catal. Today*, 1993, vol. 18, p. 209.
5. Guczi, L., van Santen, R.A., and Sayma, K.V., *Catal. Rev.-Sci. Eng.*, 1996, vol. 38, p. 249.
6. Lunsford, J., *Catal. Today*, 1990, vol. 6, p. 235.
7. Wang, L., Tao, L., Xie, M., *et al., Catal. Lett.*, 1993, vol. 21, no. 1, p. 35.
8. Xu, Y., Liu, S., Wang, L., *et al., Catal. Lett.*, 1995, vol. 30, no. 1, p. 135.
9. Solymosi, F., Erdohelyi, A., and Szoke, A., *Catal. Lett.*, 1995, vol. 32, no. 1, p. 43.
10. Solymosi, F., Szoke, A., and Cserenyi, J., *Catal. Lett.*, 1996, vol. 39, no. 1, p. 157.
11. Szoke, A. and Solymosi, F., *Appl. Catal. A: Gen.*, 1996, vol. 142, no. 1, p. 142.
12. Solymosi, F., Cserenyi, J., Szoke, A., *et al., J. Catal.*, 1997, vol. 165, no. 1, p. 156.
13. Wang, D., Lunsford, J.H., and Rosynek, M.P., *J. Catal.*, 1997, vol. 169, no. 2, p. 347.
14. Wang, D., Rosynek, M.P., and Lunsford, J.H., *Top. Catal.*, 1996, vol. 3, p. 289.
15. Wang, S.-T., Xu, Y., Wang, L., *et al., Catal. Lett.*, 1996, vol. 38, no. 2, p. 39.
16. Xu, Y., Shu, Y., Liu, S., *et al., Catal. Lett.*, 1995, vol. 35, p. 233.
17. Liu, S., Dong, Q., Ohnishi, R., and Ichikawa, M., *J. Chem. Soc. Chem. Commun.*, 1997, p. 1455.
18. Liu, S., Dong, Q., Ohnishi, R., and Ichikawa, M., *Chem. Commun.*, 1998, p. 1217.
19. User Manual of Technos EXAFS Analyzing Program.
20. Liu, W., Xu, Y., Wong, S.-T., *et al., J. Mol. Catal. A: Chem.*, 1997, vol. 120, p. 257.
21. Bsaila, M.R., Kanter, T.R., and Rhee, K.H., *Nature*, 1964, vol. 68, p. 3197; Poncelet, G. and Dubu, M.L., *J. Catal.*, 1978, vol. 52, no. 2, p. 321.
22. Mirodetos, C. and Barthomeuf, D., *J. Catal.*, 1979, vol. 57, no. 1, p. 136.
23. Lee, J.S. and Boudart, M., *Catal. Lett.*, 1993, vol. 20, no. 1, p. 97.
24. Lee, J.S., Locatelli, S., Oyama, S.T., and Boudart, M., *J. Catal.*, 1990, vol. 125, no. 1, p. 157.
25. Ozin, G.A., Prokorowitcz, P.A., and Ozkar, S., *J. Am. Chem. Soc.*, 1992, vol. 114, p. 8957.
26. Olson, D.H., Lago, R.M., and Haag, W.O., *J. Catal.*, 1980, vol. 61, no. 2, p. 390; Lago, R.M., Haag, W.O., and Mikovsky, R.J., *Stud. Surf. Sci. Catal.*, 1986, vol. 28, p. 661.